

Rotational State Distribution of CO₂ after a Collision with H Atom

Yoo Hang Kim and Seong Hoon Kim

Department of Chemistry, Inha University, Incheon 402-751, Korea

Received April 14, 1995

Based on the collisional time correlation function (CTCF) formalism, Kim and Micha derived a simple expression which gives nascent rotational state distribution of molecules after collision with fast atoms.³² The expression is valid when the collision time is short and the collision is impulsive in nature. This expression has been applied to analyze the experimentally measured, state resolved rotational distribution of CO₂ in various types of vibrational levels, *i.e.*, (00⁰1), (01¹1), (00⁰2), and (10⁰0/02⁰0). The theoretical distributions obtained from this CTCF based expression can represent the experimentally measured rotational distributions remarkably well, and have been found to be much superior to those obtained from other simple theories such as Boltzmann distribution, prior distribution, breathing ellipsoid model, and phase space statistical calculation.

Introduction

State resolved vibrational and rotational excitations resulting from the collisions between hot hydrogen atom and diatomic or triatomic molecules continues to be of great interest to both experimentalists and theoreticians alike.^{1,2} Hydrogen atoms with large, well defined kinetic energy around 1 to 3 eV are generated by laser photolysis of small hydrogen compounds such as HBr, HI and H₂S.³ These nearly monoenergetic, hot atoms are then led to collide with the target molecules, and the resulting nascent vibrationally and/or rotationally excited state populations of the scattered molecules are probed with a variety of experimental techniques.⁴

Since hydrogen atom has no internal degrees of freedom, the only possible energy transfer channels are of translation to vibration and/or rotation types ($T \rightarrow V$, R) and other complicating channels such as $V/R \rightarrow V/R$ cannot occur. This fact greatly simplifies the experimental analysis of the product quantum states. Especially interesting from a theoretical point of view are those collision systems for which product rotational state distributions are well resolved, such as $H + CO$,^{4,5} $H + CO_2$,⁶⁻¹⁴ $D + CO_2$,¹⁵ $H + NO$,¹⁶ and $H + H_2O$.¹⁷

There are many theoretical methods available which can be employed to predict or analyze the final vibrational and/or rotational distribution of the product molecules. They cover the whole spectrum in complexity and difficulty from classical to quantal and from dynamical to statistical treatments. If a very accurate potential energy surface is available, one can perform classical or quasiclassical trajectory calculations.^{18,19} In most cases, however, potential energy surfaces which are accurate enough for extensive trajectory studies are very rare. The other methods one can employ to explain the experimental rovibrational state distribution of the scattered molecules are statistical and based on simple Boltzmann type distributions, breathing ellipsoid model,^{11,12} surprisal analysis,²⁰⁻²³ or phase space theory.^{24,25}

There is another, quite simple way to tackle this problem, which is through the collisional time correlation function (CTCF) formalism.²⁶⁻³¹ Based on this formalism Kim and Micha derived several simple expressions which can be used to analyze the experimental rotational distribution of the molecules with zero³² or non-zero³³ internuclear axial component of the total electronic angular momentum after collisions with fast, monoenergetic atoms. These expressions can

be applied to molecules with a thermal distribution of initial rotational states, and are valid when the collisions are short and repulsive in nature. They applied these expressions to $H + CO$,^{32,34} $H + CO_2$,³² and $H + NO$ ³³ collision systems and obtained excellent agreement with the experimental results. When the collisions are not fully repulsive in nature, they were forced to invoke a supplemental statistical distribution based on surprisal analysis in order to satisfactorily explain the experimental results.^{32,34}

In this work, we apply the CTCF based expression to $H + CO_2$ collision system in which the rotational state distributions for many final vibrational states, (00⁰1),⁶⁻¹¹ (01¹1),¹² (10⁰0/02⁰0),¹³ and (00⁰2)¹⁴ have been reported in detail. In fact this system is experimentally most extensively studied one. Since many vibrational states having different character (symmetrical stretch, antisymmetrical stretch, bending, and overtone) are involved, this system offers a good opportunity to test our theory.

Theory

Since the essential features of the collisional time correlation function (CTCF) formalism and the procedures for deriving the cross section for scattering into a final rotational state J' are given in detail elsewhere,³² we present here only the brief summary of the theory which is necessary to interpret the experimental rotational distribution.

According to the CTCF formalism, the double differential cross section σ with respect to scattering angle Ω and the amount of energy transfer ϵ is given by

$$\frac{d^2\sigma}{d\epsilon d\Omega} = \frac{d\sigma_{av}}{d\Omega} \left(\frac{2}{\pi} \right)^{1/2} \langle (\Delta\epsilon)^2 \rangle^{-1/2} \exp \left\{ -(\epsilon - \langle \epsilon \rangle)^2 / [2 \langle (\Delta\epsilon)^2 \rangle] \right\} \quad (1)$$

where $\langle \epsilon \rangle$ is the average energy transfer and $\langle (\Delta\epsilon)^2 \rangle$ is the square of its dispersion.

Typical collision experiments with fast H atoms have been carried out using target molecules initially at thermal equilibrium. They can be analyzed for specific electronic vibrational transitions, for which the final rotational distributions are presented as functions of the final rotational energy $E_{J'}$ or quantum number (J') rather than as a function of the amount of energy transfer ϵ as in Eq. (1). Therefore, one should modify Eq. (1) to obtain an expression in terms of

E_r' , for a cross section which has been averaged over the initial rotational state distribution. Treating the initial rotational quantum number J as a continuous variable, one obtains

$$\frac{d^2\sigma}{dE_r'd\Omega} = \int_0^\infty \frac{d^2\sigma}{d\epsilon d\Omega} \left(\frac{d\epsilon}{dE_r'} \right) w_r(J) dJ. \quad (2)$$

Here unprimed and primed quantities refer to the initial and final states, respectively, and w_r refers to the distribution of initial rotational quantum numbers J . We separate the total energy E_{tot} into electronic vibrational plus rotational terms, and obtain the following relations

$$\epsilon = (E_{ev}' + E_r') - (E_{ev} + E_r) = \epsilon_{ev} + \epsilon_r \quad (3a)$$

$$\epsilon_{ev} = E_{ev}' - E_{ev} \quad (3b)$$

$$\epsilon_r = E_r' - E_r \quad (3c)$$

$$w_r = (2J+1) \exp[-E_r/(k_B T)] \quad (3d)$$

$$E_r = Bhc[J(J+1)], \quad (3e)$$

where B is the rotational constant of the molecule, h the Planck constant, and c the speed of light.

For hyperthermal collisions for which the kinetic energy is in the range of a few eVs, most of the transferred energy goes into electronic and vibrational excitation and only a small fraction goes into rotational excitation. Hence the collisions are rotationally quasielastic so that, for a given electronic vibrational transition, one can use Eq. (1) in what follows, letting

$$\epsilon - \langle \epsilon \rangle = \epsilon_r - \langle \epsilon_r \rangle, \quad \langle (\Delta\epsilon)^2 \rangle = \langle (\Delta\epsilon_r)^2 \rangle. \quad (4)$$

Then Eq. (2) becomes

$$\begin{aligned} \frac{d^2\sigma}{dE_r'd\Omega} &= \frac{d\sigma_{ev}}{d\Omega} \left(\frac{2}{\pi} \right)^{1/2} \langle (\Delta\epsilon_r)^2 \rangle^{-1/2} \\ &\times \int_0^\infty \exp[-(\epsilon_r - \langle \epsilon_r \rangle)^2 / 2\langle (\Delta\epsilon_r)^2 \rangle] (2J+1) e^{-E_r/(k_B T)} dJ, \end{aligned} \quad (5)$$

where ϵ_r depends on J .

Introducing the following dimensionless parameters and variables

$$a_2 = \langle (\Delta\epsilon_r)^2 \rangle / (k_B T)^2, \quad (6a)$$

$$x = E_r / (k_B T) \quad (6b)$$

the integral in Eq. (5) reduces to a simple form

$$I = b^{-1} \int_0^\infty \exp\left[-\left(\frac{z-x}{\sqrt{2a_2}}\right)^2\right] \exp(-x) dx, \quad (7)$$

where the parameters b and z are defined as

$$b = Bhc / (k_B T) \quad (8a)$$

$$z = (E_r' - \langle \epsilon_r \rangle) / (k_B T). \quad (8b)$$

The integral I can be evaluated analytically to obtain

$$I = (\sqrt{a_2}/b) \exp\left(\frac{a_2}{2} - z\right) \left(\frac{\pi}{2}\right)^{1/2} \operatorname{erfc}(t), \quad (9)$$

where $\operatorname{erfc}(t)$ is the coerror function of argument

$$t = (a_2 - z) / \sqrt{2a_2}. \quad (10)$$

Therefore, the double differential cross section as a function of the final rotational energy E_r' is given by

$$\begin{aligned} \frac{d^2\sigma}{dE_r'd\Omega} &= (Bhc)^{-1} \frac{d\sigma_{ev}}{d\Omega} \exp\left(\frac{a_2}{2} + \frac{\langle \epsilon_r \rangle}{k_B T} - \frac{E_r'}{k_B T}\right) \\ &\operatorname{erfc}\left[\frac{1}{\sqrt{2a_2}}\left(a_2 + \frac{\langle \epsilon_r \rangle}{k_B T} - \frac{E_r'}{k_B T}\right)\right] \\ &= A \exp\left(a_1 + \frac{a_2}{2} - x'\right) \operatorname{erfc}[(a_1 + a_2 - x')/\sqrt{2a_2}] \\ &= A f(x') \end{aligned} \quad (11)$$

where A is the combination of all the preexponential terms in Eq. (11), and a_1 and x' are dimensionless quantities defined as

$$a_1 = \langle \epsilon_r \rangle / (k_B T), \quad (12a)$$

$$x' = E_r' / (k_B T) = J'(J'+1)Bhc / (k_B T). \quad (12b)$$

Equation (11) gives a compact expression for the double differential cross section, which can be applied to cases where angular distributions have been measured. It is not any longer a Gaussian distribution, but instead a distribution of E_r' values that peaks at intermediate value of x' and tapers off at both small and large x' .

A similar expression can be adopted to interpret gas phase experiments by integration over scattering angles. Integrating Eq. (11) over the solid angle Ω and assuming that the dependences of a_1 and a_2 on scattering angles are weak for hyperthermal collisions, one obtains

$$\frac{d\sigma}{dE_r'} = \int \frac{d^2\sigma}{dE_r'd\Omega} d\Omega = \left(\int A d\Omega \right) f(x') = A' f(x'), \quad (13)$$

where A' is another constant independent of E_r' .

Finally, the scattering cross section for the final rotational state J' can be obtained by numerical integration,

$$\begin{aligned} \sigma(J') &= Bhc \int_{J'-1/2}^{J'+1/2} \left(\frac{d\sigma}{dE_r'} \right) (2J'+1) dJ' \\ &\approx A' f[x'(J')] (2J'+1). \end{aligned} \quad (14)$$

Therefore, $\sigma(J')$ can be expressed as a function of the final rotational quantum number J' and of three parameters a_1 , a_2 , and a_3 as follows:

$$\begin{aligned} \sigma(J') &= a_3 (2J'+1) \exp\left(a_1 + \frac{a_2}{2} - x'\right) \\ &\times \operatorname{erfc}[(a_1 + a_2 - x')/\sqrt{2a_2}] \end{aligned} \quad (15)$$

with x' given by Eq. (12b)

The essential features of the final rotational distribution are determined solely by the parameters a_1 and a_2 . The third parameter a_3 is a scaling factor which is necessary to fit the experimental distribution usually expressed in an arbitrary, relative scale.

In order to test our approach, we could proceed in two ways. The first would be to calculate the three parameters a_i from first principles and to predict the final rotational distribution. This would require detailed knowledge of the interaction potential and extensive trajectory calculations.

The second way, which is less rigorous but much easier, would be to fit the theoretical curve to the experimental

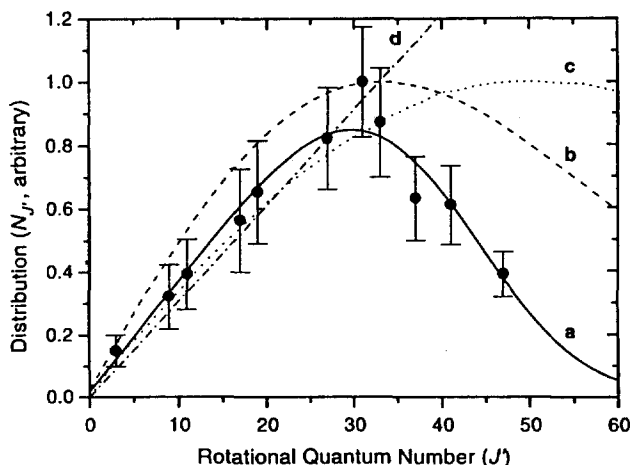


Figure 1. Rotational distribution of CO₂ (00⁰₁). ● experiment (Ref. 7); curve **a**, this work (CTCF); curve **b**, Boltzmann distribution, $T=1270$ K (Ref. 7); curve **c**, phase space statistical calculation (Ref. 13); curve **d**, prior distribution (Ref. 7).

data to see whether the functional form of our distribution is satisfactory, and also to compare the energy quantities obtained from the best fit to those from the experiment. In view of the simple nature of our approach, here we choose the second procedure to test the derived distribution, and proceed as follows.

From the experimental rotational distribution, one obtains the relative population for each J' and minimizes a chi square function of the parameters $\{a_i, i=1 \text{ to } 3\} = \mathbf{a}$ defined by

$$\chi^2(\mathbf{a}) = \sum_{J'} \left[\frac{N_J' - N(J'; \mathbf{a})}{\Delta N_J'} \right]^2, \quad (16)$$

where N_J' is the experimental relative population for final rotational state J' , $\Delta N_J'$ is the standard deviation in the measured values of N_J' , and $N(J'; \mathbf{a})$ is the theoretical distribution for a given set of the parameters \mathbf{a} . The computer program we have used requires $\Delta N_J'$'s as input together with J' and N_J' . In cases where $\Delta N_J'$'s are not reported in the experiment, a constant percentage value has been assigned to all N_J' 's. The actual magnitude of the constant itself, however, does not affect the final result.

We have used the numerical procedure of Levenberg Marquardt,³⁵⁻³⁷ to obtain the best fit parameters. The iterative process to obtain the best set of \mathbf{a} values was carried out until two successive iterations gave $\chi^2(\mathbf{a})$'s within 10^{-3} of each other.

Results and Discussion

In a number of papers⁶⁻¹⁴ Flynn, Weston, Jr., and their coworkers determined the detailed rotational state distribution of various vibrational levels of CO₂ after collisions with hot H (or D) atoms. They first obtained hot H atom ($E_k=2.3$ eV) by UV photolyzing ($\lambda=193$ nm) H₂S molecules. The hot H atoms are then led to collide with CO₂ (00⁰₀) whose initial rotational states are in equilibrium with the experimental temperature (T) to produce the rovibrationally excited CO₂ (mn^p, J') probed by time resolved diode laser spectroscopy.

We applied our CTCF based expression, i.e., Eq. (15), to

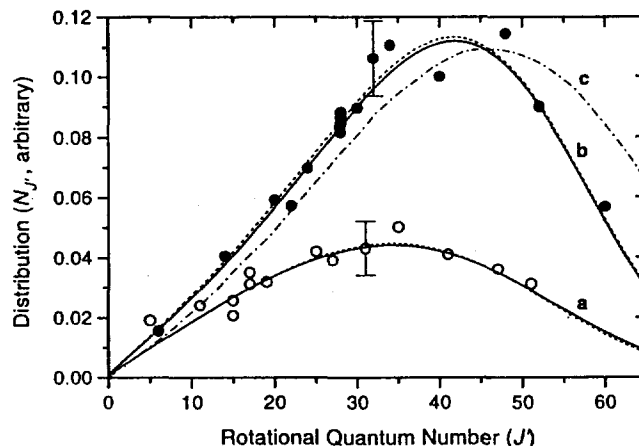


Figure 2. Rotational distribution of CO₂ (01¹₁). ○ (odd J'), ● (even J') experiment (Ref. 12); curves **a**, this work (CTCF) for odd J' , curves **b**, for even J' . — when the same value of errors are assumed, ... when the same percentage errors are assumed; curve **c**, breathing ellipsoid model for even J' (Ref. 12).

the experimental data and obtained the best fit curves by use of the iteration method mentioned in the previous section. Here, we report our theoretical analysis results for the nascent rotational state (J') distribution of CO₂ in the final vibrational levels (00⁰₁), (01¹₁), (00⁰₂), and (10⁰₀/02⁰₀).

CO₂ (00⁰₁). The rotational state measurements for the final antisymmetric stretching vibrational state (00⁰₁) are reported in a series of papers.⁶⁻¹⁰ We used the data given in Ref. 7 for our theoretical analysis since only there experimental error limits are given for every data point. The results are presented in Figure 1 together with those predicted from some other simple theories. From the figure it is quite evident that the CTCF based expression can satisfactorily represent the measured rotational distribution. Other simple distributions such as Boltzmann distribution ($T=1270$ K), phase space statistical calculation,¹³ and prior distribution⁷ can not represent the measured distribution very well. Especially, they all fail and give grossly overestimated distribution when the final rotational quantum numbers (J') are large.

Our best fit parameters for (00⁰₁) state are $a_1 = -0.678$, $a_2 = 4.34$ and $a_3 = 0.0499$. Besides the general shape of the theoretical distribution curve, rotational quantum number at which the distribution shows its maximum (J'_{\max}), average rotational quantum number $\langle J' \rangle$, average rotational energy $\langle E_{J'} \rangle$ and its dispersion $\langle (\Delta E_{J'})^2 \rangle^{1/2}$ can be used to characterize both the theoretical and the experimental distribution and/or to judge the goodness of the fit.

For this vibrational state J'_{\max} , $\langle J' \rangle$, $\langle E_{J'} \rangle$ and $\langle (\Delta E_{J'})^2 \rangle^{1/2}$ are 31, 27, 7.16×10^{-21} joule, and 4.63×10^{-21} joule for the experimental distribution and 29, 29, 8.17×10^{-21} joule, and 6.27×10^{-21} joule, respectively for the CTCF based theoretical distribution. The two sets of characterizing parameters agree with each other quite well.

CO₂ (01¹₁). The final rotational distribution in the combination bend stretch (01¹₁) vibrational state is given in Figure 2. In this vibrational state both even and odd rotational states are possible, and the experimentally observed distribution shows even-odd oscillations. These oscillations are a consequence of the doubling of rotational levels due to

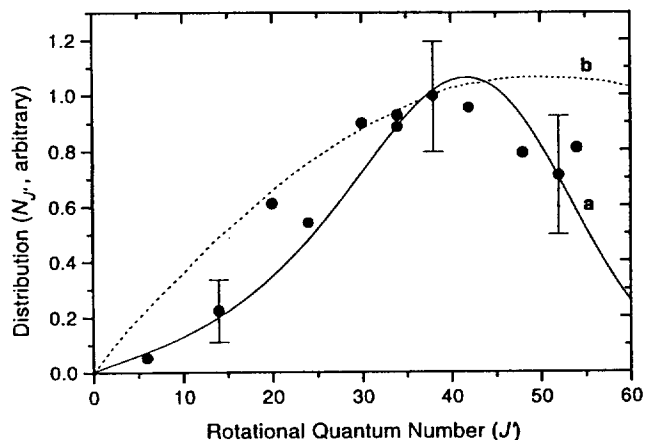


Figure 3. Rotational distribution of CO₂ (00⁰₂). ● experiment (Ref. 14); curve **a**, this work (CTCF); curve **b**, phase space statistical calculation (Ref. 14).

coupling between the nuclear rotational motion and the degenerate bending vibrations in CO₂, and the requirement that the nuclear spin rovibrational wave function of CO₂ be symmetric with respect to exchange of oxygen nuclei.¹² Clary *et al.* calculated similar oscillations for low energy rovibrationally inelastic scattering between He and CO₂.^{38–40} The first experimental observation of this phenomenon was made by Herschberger *et al.* in CO₂ (01¹₀) state.⁴²

Since only one error bar is given to both odd and even experimental distributions and our fitting procedure requires error limits for all data points, we tried two different approaches in actual fitting. In one approach we assigned the same absolute value of error, while in the other the same percentage error to all the data points.

As can be seen from Figure 2, the two approaches give essentially the same results and reproduce the experimental distribution very well. Therefore, in further discussion, we present the results only for the theoretical distribution for which the same percentage errors are assigned. Also shown in Figure 2 is another theoretical distribution (curve c) for even J' rotational states predicted by the breathing ellipsoid model,^{11,12} which is in rather poor agreement with the experimental distribution compared with this work. The fitting and energy parameters for CTCF based theoretical distribution are as follows. Odd J' distribution: $a_1 = -2.66$, $a_2 = 17.7$, $a_3 = 0.0054$; $J'_{\max} = 35$ (35), $\langle J' \rangle = 33$ (27), $\langle E_r' \rangle = 1.07 \times 10^{-20}$ (7.28×10^{-21}) joule, $\langle (\Delta E_r')^2 \rangle^{1/2} = 7.97 \times 10^{-21}$ (9.33×10^{-21}) joule. Even J' distribution: $a_1 = 1.01$, $a_2 = 9.97$, $a_3 = 0.0061$; $J'_{\max} = 42$ (48), $\langle J' \rangle = 38$ (32), $\langle E_r' \rangle = 1.31 \times 10^{-20}$ (8.87×10^{-21}) joule, $\langle (\Delta E_r')^2 \rangle^{1/2} = 8.21 \times 10^{-21}$ (6.27×10^{-21}) joule. The values in parentheses are those for the experimental distribution.

CO₂ (00⁰₂). Khan *et al.* reported the nascent rotational distribution of CO₂ in the overtone antisymmetric stretch vibrational state after collision with fast H atom,^{7,14} and their experimental data are presented in Figure 3. Also shown in the same figure are the theoretical distribution curves obtained from CTCF based expression and from phase space statistical calculation.¹⁴ It is evident from the figure that the former reproduces the experimental distribution much better than the latter. In fitting Eq. (15) to the measured distribu-

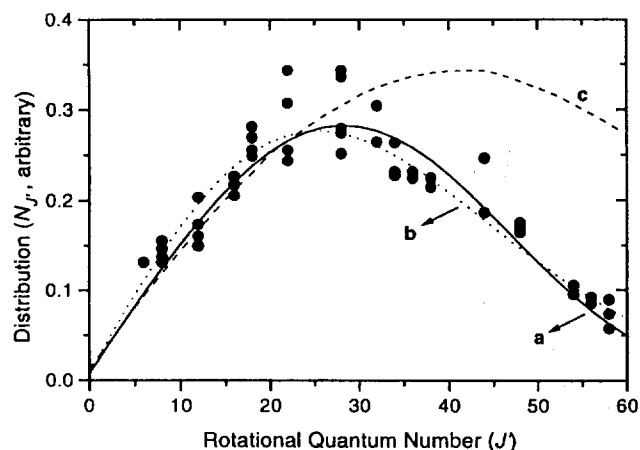


Figure 4. Rotational distribution of CO₂ (10⁰₀/02⁰₀). ● experiment (Ref. 13); curve **a**, this work (CTCF); curve **b**, Boltzmann distribution, $T_r = 747$ K (Ref. 13); curve **c**, phase space statistical calculation (Ref. 13).

tion, we used the error limits when available. When they are not available, we assigned percentage errors which vary gradually according to the rotational quantum number between the values explicitly given in the figure.

The fitting parameters for Eq. (15) are $a_1 = 1.92$, $a_2 = 3.77$, and $a_3 = 0.0354$. The quantum numbers and energy parameters which characterize the theoretical and experimental distributions are as follows. As before, the values in parentheses are those for the experimental distribution.

$J'_{\max} = 42$ (38), $\langle J' \rangle = 38$ (38), $\langle E_r' \rangle = 1.23 \times 10^{-20}$ (1.20×10^{-20}) joule, $\langle (\Delta E_r')^2 \rangle^{1/2} = 6.69 \times 10^{-21}$ (6.40×10^{-21}) joule. The two sets of the values agree with each other extremely well.

CO₂ (10⁰₀/02⁰₀). In Figure 4 are shown the experimentally observed nascent rotational distribution of CO₂ in the Fermi mixed symmetric stretch/overtone bend vibrational level.¹³ Three types of theoretical distributions are also presented in the same figure. The experimental distribution peaks at $J' \approx 26$ and is quite well fit by 747 K Boltzmann distribution and also by CTCF based expression (this work). The phase space statistical calculation, however, does not represent the measured distribution well. In fitting Eq. (15) to the experimental distribution we assigned the same 20 % error to all the data points. We deem this error reasonable, and think that the calculated distribution will not be affected very much by the actual value of the error limits. This has been verified in the case of CO₂ (01¹₁) distribution. The fitting parameters for Eq. (15) are $a_1 = -5.10$, $a_2 = 17.0$, and $a_3 = 0.0648$.

Even though the Boltzmann and the CTCF distributions look qualitatively almost the same, their relative superiority can be judged by the energy characteristics. Experimental distribution: $J'_{\max} = 26$, $\langle J' \rangle = 28$, $\langle E_r' \rangle = 7.52 \times 10^{-21}$ joule, $\langle (\Delta E_r')^2 \rangle^{1/2} = 6.51 \times 10^{-21}$ joule. CTCF distribution: $J'_{\max} = 28$, $\langle J' \rangle = 30$, $\langle E_r' \rangle = 9.09 \times 10^{-21}$ joule, $\langle (\Delta E_r')^2 \rangle^{1/2} = 7.57 \times 10^{-21}$ joule. Boltzmann distribution (747 K): $J'_{\max} = 26$, $\langle J' \rangle = 28$, $\langle E_r' \rangle = 1.03 \times 10^{-20}$ joule, $\langle (\Delta E_r')^2 \rangle^{1/2} = 1.03 \times 10^{-20}$ joule. Therefore, the CTCF distribution is slightly better than the Boltzmann distribution in representing the experimental distribution.

Conclusion

The collisional time correlation function based expression has been applied to analyze the nascent rotational state distribution of CO₂ in several vibrational states after collision with fast H atom. The simple expression can represent the experimentally observed rotational distribution in the different types of vibrational levels, (00⁰1), (01¹1), (00⁰2) and (10⁰0/02⁰0) remarkably well. The CTCF distribution has also been found to be superior to other distributions derived from other simple theories such as Boltzmann distribution, prior distribution, breathing ellipsoid model, and phase space statistical calculation.

Acknowledgments. The present studies were supported by the Basic Science Research Institute Program, Ministry of Education, 1994 (Project No. BSRI-94-3428).

References

1. Flynn, G. W.; Weston Jr., R. E. *Annu. Rev. Phys. Chem.* **1986**, *37*, 551.
2. Weston, Jr., R. E.; Flynn, G. W. In *Advances in Chemical Kinetics and Dynamics*, Vol. 2, *Vibrational Energy Transfer Involving Large and Small Molecules*; Barker, J. R., Ed.; Jai Press: Greenwich, U.S.A., 1994.
3. Wight, C. A.; Leone, S. R. *J. Chem. Phys.* **1983**, *78*, 4875.
4. Chawla, G. K.; McBane, G. C.; Houston, P. L.; Schatz, G. C. *J. Chem. Phys.* **1988**, *88*, 5481 and references therein.
5. McBane, G. C.; Kable, S. H.; Houston, P. L.; Schatz, G. C. *J. Chem. Phys.* **1991**, *94*, 1141.
6. O'Neil, J. A.; Wang, C. X.; Cai, J. Y.; Flynn, G. W.; Weston Jr., R. E. *J. Chem. Phys.* **1986**, *85*, 4195.
7. O'Neil, J. A.; Wang, C. X.; Cai, J. Y.; Flynn, G. W.; Weston Jr., R. E. *J. Chem. Phys.* **1988**, *88*, 6240.
8. Khan, F. A.; Kreutz, T. G.; Zhu, L.; Flynn, G. W.; Weston Jr., R. E. *J. Phys. Chem.* **1988**, *92*, 6171.
9. Kreutz, T. G.; Khan, F. A.; Flynn, G. W. *J. Chem. Phys.* **1990**, *92*, 347.
10. Khan, F. A.; Kreutz, T. G.; Flynn, G. W.; Weston Jr., R. E. *J. Chem. Phys.* **1990**, *92*, 4876.
11. Kreutz, T. G.; Flynn, G. W. *J. Chem. Phys.* **1990**, *92*, 452.
12. Khan, F. A.; Kreutz, T. G.; O'Neil, J. A.; Wang, C. X.; Flynn, G. W.; Weston Jr., R. E. *J. Chem. Phys.* **1990**, *93*, 445.
13. Hewitt, S. A.; Herschberger, J. F.; Chou, J. Z.; Flynn, G. W.; Weston, Jr., R. E. *J. Chem. Phys.* **1990**, *93*, 4922.
14. Khan, F. A.; Kreutz, T. G.; Flynn, G. W.; Weston, Jr., R. E. *J. Chem. Phys.* **1993**, *98*, 6183.
15. Hewitt, S. A.; Herschberger, J. F.; Flynn, G. W.; Weston Jr., R. E. *J. Chem. Phys.* **1987**, *87*, 1894.
16. Wight, C. A.; Donaldson, D. J.; Leone, S. R. *J. Chem. Phys.* **1985**, *83*, 660.
17. Lovejoy, C. M.; Goldfarb, L.; Leone, S. R. *J. Chem. Phys.* **1992**, *96*, 7180.
18. For Example, Schatz, G. C.; Fitzcharles, M. S.; Harding, L. B. *Faraday Discuss. Chem. Soc.* **1987**, *84*, 359.
19. Schatz, G. C.; Fitzcharles, M. S. In *Selectivity In Chemical Reactions*, Whitehead, J. C., Ed.; Kluwer: Dordrecht, 1988; pp. 353-365.
20. Kinsey, J. L. *J. Chem. Phys.* **1971**, *54*, 1206.
21. Levine, R. D.; Bernstein, R. B. *Acc. Chem. Res.* **1974**, *7*, 393.
22. Levine, R. D.; Kinsey, J. L. In *Atom Molecule Collision Theory*; Bernstein, R. B., Ed.; Plenum: New York, U.S.A., 1979; Chap. 22.
23. Bernstein, R. B. *Chemical Dynamics via Molecular Beam and Laser Techniques*; Clarendon, Oxford, 1982; p 196.
24. Pechukas, P.; Light, J. C. *J. Chem. Phys.* **1965**, *42*, 3281.
25. Light, J. C. *Discuss. Faraday Soc.* **1967**, *44*, 14.
26. Micha, D. A. *Int. J. Quantum Chem.* **1986**, *S20*, 773.
27. Micha, D. A. *Int. J. Quantum Chem.* **1981**, *S15*, 643.
28. Micha, D. A. *J. Chem. Phys.* **1979**, *70*, 3165.
29. Micha, D. A. *J. Chem. Phys.* **1979**, *70*, 565.
30. Micha, D. A. *Chem. Phys. Lett.* **1977**, *46*, 188.
31. Vilallonga, E.; Micha, D. A. *Phys. Rep.* **1992**, *212*, 329. Micha, D. A.; Vilallonga, E. F. *Adv. Chem. Phys.* **1993**, *LXXXIV*, 1.
32. Kim, Y. H.; Micha, D. A. *J. Chem. Phys.* **1989**, *90*, 5486.
33. Kim, Y. H.; Micha, D. A. *Bull. Kor. Chem. Soc.* **1995**, *16*, 436.
34. Kim, Y. H.; Lee, Y. J. *Bull. Bas. Sci. Inst. Inha Univ.* **1995**, *16*, 161.
35. Press, W. T.; Flannery, B. P.; Teukolsky, S. A.; Vetterling, W. T. *Numerical Recipes-The Art of Scientific Computing* (Cambridge University, Cambridge, 1986), p 521-528.
36. Vetterling, W. T.; Teukolsky, S. A.; Press, W. T.; Flannery, B. P. *Numerical Recipes Example Book (Fortran)* (Cambridge University, Cambridge, 1985), p 155-157.
37. Note: The subroutine MRQMIN listed in Ref. 23 should be slightly modified to prevent premature termination of the iterative process after an increase in χ^2 . All one has to do is to omit the fourth from the last statement (CHISQ=OCHISQ) from the subroutine program.
38. Clary, D. C. *Chem. Phys. Lett.* **1980**, *74*, 454.
39. Clary, D. C. *J. Chem. Phys.* **1983**, *78*, 4915.
40. Alexander, M. H.; Clary, D. C. *Chem. Phys. Lett.* **1983**, *98*, 319.
41. Banks, A. J.; Clary, D. C. *J. Chem. Phys.* **1987**, *86*, 802.
42. Herschberger, J. F.; Hewitt, S. A.; Flynn, G. W.; Weston Jr., R. E. *J. Chem. Phys.* **1988**, *88*, 7243.